Journal of Alloys and Compounds 611 (2014) 11–18

Contents lists available at ScienceDirect

Journal of Alloys and Compounds

journal homepage: www.elsevier.com/locate/jalcom

# Hydrogen sorption properties of mechanically alloyed $Mg_{1-2x}Fe_xTi_x$ powder mixtures

M. Meyer, L. Mendoza-Zélis *

*IFLP, Departamento de Física, Facultad de Ciencias Exactas, Universidad Nacional de La Plata, CC67, 1900 La Plata, Argentina*

ARTICLE INFO

*Article history:*
Received 17 March 2014
Received in revised form 14 May 2014
Accepted 15 May 2014
Available online 24 May 2014

*Keywords:*
Metallic hydrides
Hydrogen storage
Mechanical alloying
Mössbauer spectroscopy

ABSTRACT

We report an investigation on the hydrogen sorption properties of mechanically alloyed systems of nominal composition $Mg_{1-2x}Fe_xTi_x$ ($x = 0.10$, 0.15 and 0.20). The starting metallic powder mixtures were milled in $H_2$ ambient, till a steady state with no further $H_2$ absorption was attained. The resulting samples were then characterized and submitted to several $H_2$ discharge–charge cycles in order to determine their hydrogen sorption properties. With the aim to investigate the dependence of these properties on the sample microstructure we also studied samples of nominal composition $Mg_{80}Fe_{10}Ti_{10}$ obtained through different processing routes. In those samples the Fe and Ti additives were added as a fine powder mixture or as the intermetallic compound FeTi while their mechanical alloying with Mg was conducted under $H_2$ or Ar atmosphere. All the samples were characterized by X-ray diffraction and Mössbauer spectroscopy on $^{57}Fe$, before and after their cycling in $H_2$. The results are analyzed in the framework of possible mechanisms for the transition metals catalytic action on the $H_2$ sorption processes and the influence of the sample microstructure.



## 1. Introduction

Hydrogen – as an energy carrier – and solid hydrides – as hydrogen storage materials – are thought to be of crucial importance in the global energy prospects. Nanostructured and mechanically alloyed materials play a central role in the present efforts to increase the storage capacity and the rate of hydrogen charge and discharge of solid hydrides [1]. While Mg is nominally a good candidate for solid state hydrogen storage, due to its capacity, availability and low cost, its sorption kinetics should be considerably improved for it become of practical use in mobile applications [2]. The reduction of grain sizes to the nanometer scale and the addition of small quantities of transition metals, such as Fe and Ti, as catalysts, have demonstrated to be useful for that purpose [3–5].

Mg also combines with Fe and hydrogen to form the complex ternary hydride $Mg_2FeH_6$ [6] with very high volumetric hydrogen content (150 kg $H_2/m^3$). This ternary hydride contains $[FeH_6]^{-4}$ anions with ionic-covalent bonds for H atoms leading to a high dissociation enthalpy (77 kJ/mol) and has been considered as a candidate for energy storage also [7]. Since Mg and Fe are practically immiscible and do not form any compound, the complex hydride, does not have an hydrogen-free intermetallic precursor and when it decomposes Mg and Fe must mutually segregate. This complex hydride may be obtained by mechanical alloying of the metallic constituents in $H_2$ atmosphere at moderate pressure and room temperature [8–11]. Indeed, when Mg–Fe mixtures in any ratio are milled in $H_2$ atmosphere the formation of the ternary hydride occurs even for minute Fe contents [8,12]. The synthesis of complex hydrides by mechanical milling of the constituent metals in an $H_2$ ambient at room temperature, has been extended to ternary $Mg_2FeH_6$, $Mg_2CoH_5$ and $Mg_2NiH_4$ [11,13] as well as quaternary (Mg combined with two of the transition metals Fe, Co and Ni, in various proportions) systems [14].

Recently, improved hydrogen sorption kinetics was reported for $Mg_{1-2x}Fe_xTi_x$ films with $x = 0.10$, 0.15, 0.20 [15]. Since then, several studies have been reported on similar systems under the form of films [16–18] and it would be interesting to explore these properties in materials under powder form. Indeed, such an study was reported [19] on samples obtained by milling in Ar, mixtures of $MgH_2$ with elemental Fe and/or Ti or intermetallic FeTi, totalizing 10 at% of additives.

We started an investigation on mechanically alloyed Mg–Fe–Ti powder mixtures of similar composition following a different route, with the aim to test those salient sorption properties in such materials. We milled the samples in $H_2$ ambient, till a steady state with no further $H_2$ absorption was attained and followed the

* Corresponding author. Tel.: +54 221 423 0122; fax: +54 221 423 6335.
*E-mail address:* mendoza@fisica.unlp.edu.ar (L. Mendoza-Zélis).

http://dx.doi.org/10.1016/j.jallcom.2014.05.105
0925-8388/

mechanosynthesis process through the analysis of the hydrogen absorption kinetic curves. The resulting hydrides were characterized and afterwards submitted to several $H_2$ discharge–charge cycles. In order to further investigate the dependence of these properties on the sample microstructure we also studied samples of nominal composition $Mg_{80}Fe_{10}Ti_{10}$ obtained through four different processing routes. For that samples the Fe and Ti additives were added alternatively as a fine powder mixture or as the intermetallic compound FeTi, while their mechanical alloying with Mg was conducted under either $H_2$ or Ar atmosphere. All the samples were characterized by X-ray diffraction and Mössbauer spectroscopy on $^{57}$Fe, before and after their cycling in $H_2$. The results are analyzed and discussed trying to establish the dis/advantages of each preparation route and if the simultaneous presence of Fe and Ti imply a beneficial effect on their catalytic action in powder samples.

## 2. Experimental

For one group of samples, the starting pure powders: Mg (Sigma–Aldrich, 99.98), Fe (Merk, 99.5) and Ti (Cerac, 99.4) were mixed together in molar ratios adequate to the desired stoichiometry, i.e. $Mg_{80}Fe_{10}Ti_{10}$ (samples labelled MFT04 and MFT07), $Mg_{70}Fe_{15}Ti_{15}$ (MFT05) and $Mg_{60}Fe_{20}Ti_{20}$ (MFT06). Samples of 500 mg were then filled in a cylindrical steel milling vial together with one steel ball ($\Phi$ = 12 mm), giving a ball to sample mass ratio around 14:1. All sample handling was performed in a glove box under a controlled protective atmosphere, keeping the oxygen content below a few ppm by reducing it to water vapor further eliminated in a drying train. The milling chamber was connected to a gas reservoir (total volume $V$ = 20 cm$^3$) and sealed with an O-ring. After several washes of the chamber, the mechanical milling of each powder mixture was conducted in $H_2$ (N50) atmosphere using a modified Retsch horizontal mill oscillating at a fixed frequency of 32 Hz. The $H_2$ pressure, initially $P_i$ = 0.3 MPa, was measured continuously during the process with a strain gauge (Druck PDCR 4020) with 0.5 kPa sensibility (accuracy ±0.04%). To avoid a significant pressure reduction as hydrogen absorption proceeds, the system was automatically refilled with $H_2$ each time the pressure drops to 0.9$P_i$, restoring the initial pressure $P_i$ without milling interruption. The mill was stopped well after a steady state with no further $H_2$ absorption was attained [14].

From the measured $H_2$ pressure evolution, the reaction progress was monitored during milling and a kinetic curve established in each case. The instant number of absorbed hydrogen atoms per metal atom $y = N_H/N_M = -2\Delta P \cdot V \cdot M/R \cdot T \cdot m$ was evaluated from the accumulated pressure change $\Delta P$, as a function of milling time $t_m$. $R$ is the gas constant, $M$ the molar mass of the formula $Mg_{1-2x}Fe_xTi_x$ and $m$ the powder mass.

For a second group of samples, prior to their mixing with Mg in 80 Mg:10Fe:10Ti stoichiometry, Fe and Ti powders were mechanically alloyed in Ar (N50) to obtain the intermetallic FeTi (MFT08, MFT11 and MFT12) or finely dispersed by milling in Ar with three small balls (MFT09, MFT10 and MFT13). The subsequent milling with Mg was conducted either in $H_2$ ambient as described above (MFT10, MFT11, MFT12 and MFT13) or in Ar (N50) atmosphere (MFT08 and MFT09). In the former cases, kinetic curves were obtained, while no Ar gas consumption was detected for the latter.

All the obtained samples were characterized by X-ray diffraction (XRD) in Bragg geometry with a Philips PW1710 diffractometer using Cu K$\alpha$ radiation. The samples were also analyzed by Mössbauer spectrometry (MS) in transmission geometry using a $^{57}$Co *Rh* source at constant acceleration. This technique, based on the $\gamma$-rays resonant absorption by $^{57}$Fe nuclei, allows the investigation of atomic configurations in the neighborhood of Fe atoms and reveals the possible formation of Fe containing compounds or complexes. All quoted isomer shifts are relative to the Mössbauer source (Rh metal).

Afterwards, the samples were thermally cycled in $H_2$: about 100 mg of powder were charged in a reaction chamber filled with $H_2$ at a given starting pressure, heated at constant volume (14.7 ± 1 cm$^3$) up to about 720 K and then cooled down to room temperature under the same conditions. The chamber pressure and sample temperature were measured during the cycle, using strain gauges (accuracy ±0.04%) and a Pt100 thermometer (accuracy ±0.15%), respectively. The process was repeated several times at the same and at different starting pressures. The resulting $P$ vs $T$ curves were analyzed to extract approximate values of the $H_2$ desorption (absorption) pressure at the corresponding temperature, as explained below.

The evolution of $P$ vs $T$ during typical heating and cooling runs is shown respectively in Figs. 1 and 2 and compared with the corresponding curves obtained with the reactor filled with $H_2$ at similar pressures but without any sample. These *empty reactor* curves behave as $P = n_g \cdot \varphi(T)/V$ where $n_g$ is the number of $H_2$ moles, $V$ is the reactor volume and $\varphi(T)$ an empirical function that may be described as $\varphi(T) = RT/(a + bT + cT^2)$. Average fitted values are $a = 0.0718_8$; $b = 0.00334_1$; $c = -6.25_3 10^{-7}$ for heating and $a' = 0.2525_2$; $b' = 0.00244_1$; $c' = 0$ for cooling. When the reactor is heated (cooled) with an hydride sample in it, at certain temperature the pressure

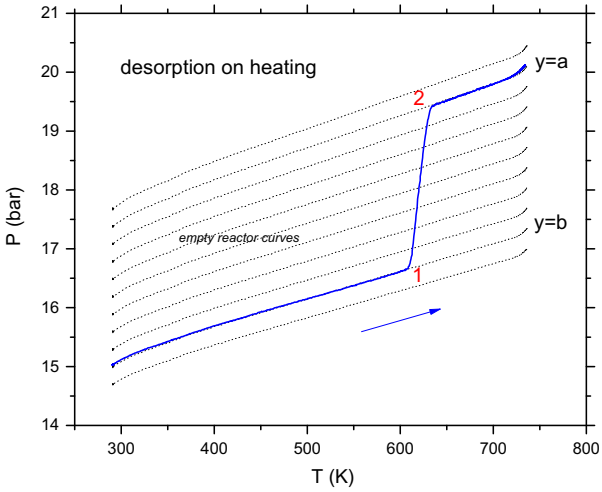


**Fig. 1.** Evolution of pressure with temperature, during the heating of a typical sample, compared with similar curves obtained without sample.

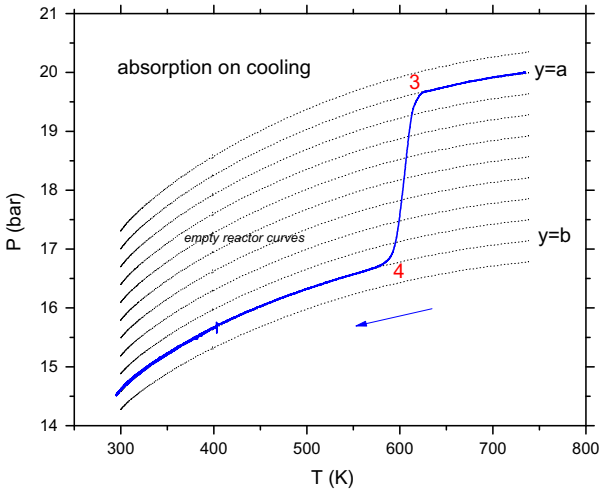


**Fig. 2.** Evolution of pressure with temperature, during the cooling of a typical sample, compared with similar curves obtained without sample.

deviates sharply from the empty reactor behavior, indicating the start of a $H_2$ desorption (absorption) process, and it recovers that behavior at a different pressure when the process is accomplished. The pressure behaves thus as $P = n_g(-y) \cdot \varphi(T)/V_g = (n_o - n_M y/2) \cdot \varphi(T)/V_g$, where $n_o$ is the total number of $H_2$ moles in the system and $V_g$ is the volume available for the gas phase which we assume constant (neglecting the volume variations of solid phases). Despite the dynamical character of the processes, we may interpret the temperature and pressure values ($T_1$, $P_1$) and ($T_3$, $P_3$) as indicative of the start of $H_2$-desorption from a charged sample ($y = b$) and $H_2$-absorption from a partially discharged one ($y = a$), respectively.

Finally, after their cycling in $H_2$, all the samples were characterized again by XRD and MS.

## 3. Results and discussion

For their presentation and discussion the results are grouped in four subsections. In 3.1 we present results about the milling of Fe–Ti equiatomic mixtures used in the preparation of some samples. Then we describe, in 3.2, the kinetic curves associated with the preparation of all the studied samples and their characterization by XRD and MS. In 3.3 we report the thermal cycling of samples and the subsequent characterization with those techniques. Finally in 3.4, we describe the results obtained from the constant volume $P$ vs $T$ curves associated with the thermal sorption cycles.

### 3.1. Mechanical pre-treatments

We will first consider the result of milling the equiatomic Fe–Ti mixtures that have been used in the preparation of the second group of samples. As expected, the mechanical milling with several small balls during 120 min, just mix the components preserving their identity as demonstrated by XRD and MS and shown in Fig. 3a and c respectively. Instead, the milling with one heavy ball during 600 min yields the intermetallic compound FeTi with mean grain size about 8 nm according to Scherrer formula (see Fig. 3b). The corresponding Mössbauer spectrum, shown in Fig. 3d, display a singlet with isomer shift $\delta = -0.275$ mm/s, characteristic of Fe in FeTi besides about 5 at% of pure Fe indicating that the reaction was not complete.

### 3.2. Mechanically synthesized samples

Some of the resulting kinetic curves for hydride formation during milling, are shown in Figs. 4 and 5, normalized to their steady state value $y_{SS}$. All the kinetic curves reach a steady state, after some hours of milling, with an average H composition of the solid phases, $y = n_H/n_M$, close to 2 (see Table 1). Note that this is indicative of almost complete reactions, as all the expected phases: $MgH_2$, $TiH_2$ and $Mg_2FeH_6$ have 2 hydrogen per metal atom.

As previously reported [13], the kinetic curve for Mg–Fe mixtures shows a complex shape as a result of a two stage process: the prior formation of $MgH_2$ (fast process) that in turn reacts with Fe to form the complex hydride $Mg_2FeH_6$ (slow process). On his hand, the milling of pure Ti in $H_2$ lead to the fast formation of $TiH_2$ [20] through a mechanically assisted reaction that completes, under the same experimental conditions, in less than 20 min [21,22]. With one exception described below, the kinetic curves for the present samples also show the complex shape with a shoulder, characteristic of the two stage formation of $Mg_2FeH_6$. As shown in Fig. 4, the shoulder is less pronounced in the samples

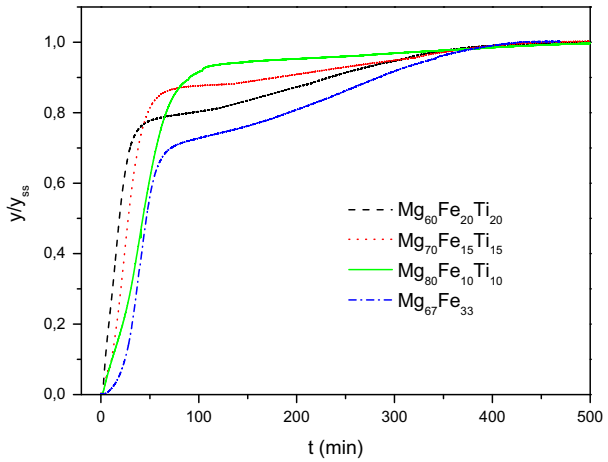


**Fig. 4.** Number of absorbed hydrogen atoms per metal atom $y = N_H/N_M$ normalized to its steady state value $y_{SS}$, as a function of milling time $t_m$ for several studied samples, including for comparison a $Mg_{67}Fe_{33}$ one.

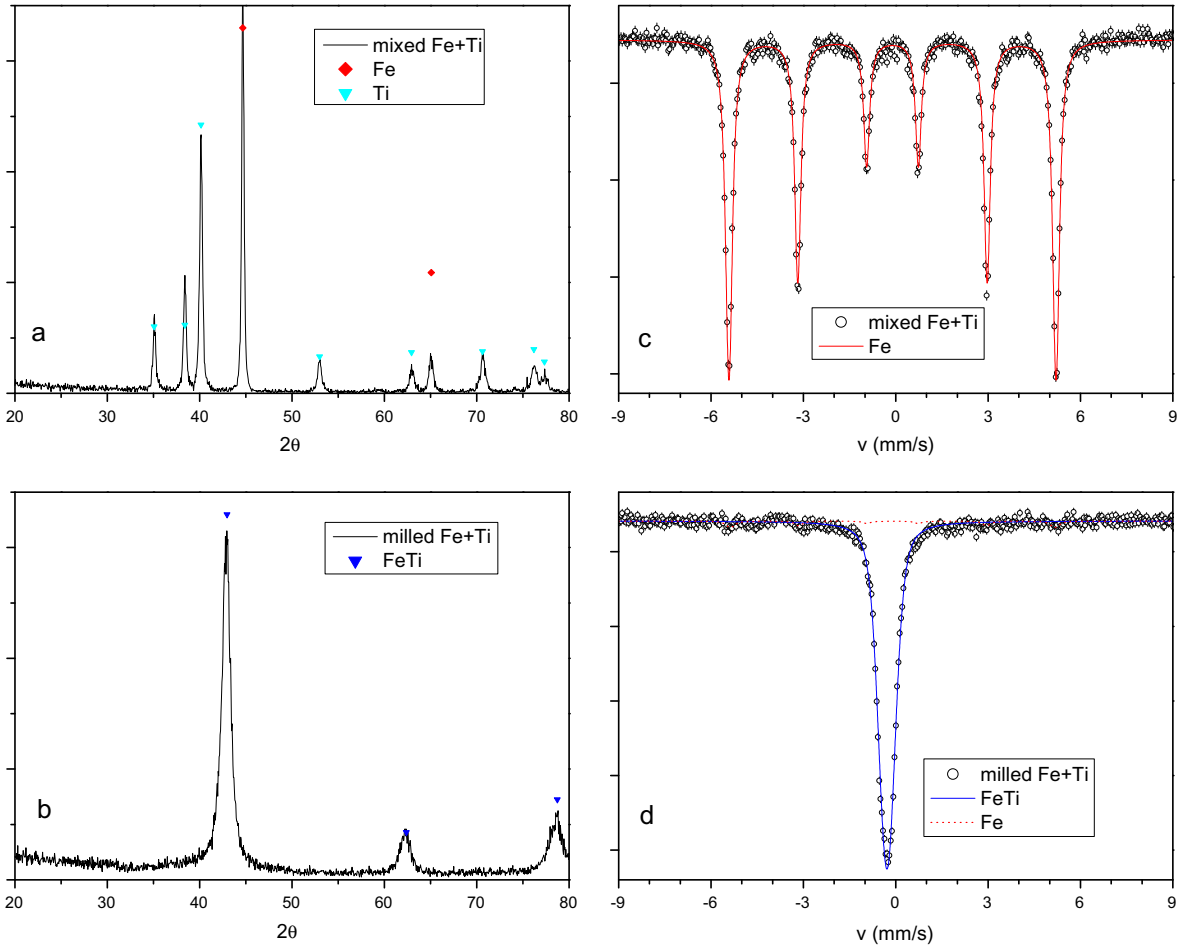


**Fig. 3.** X-ray diffraction patterns and Mössbauer spectra of equiatomic Fe–Ti mixtures mechanically mixed (a) and (c) and mechanically alloyed (b) and (d).

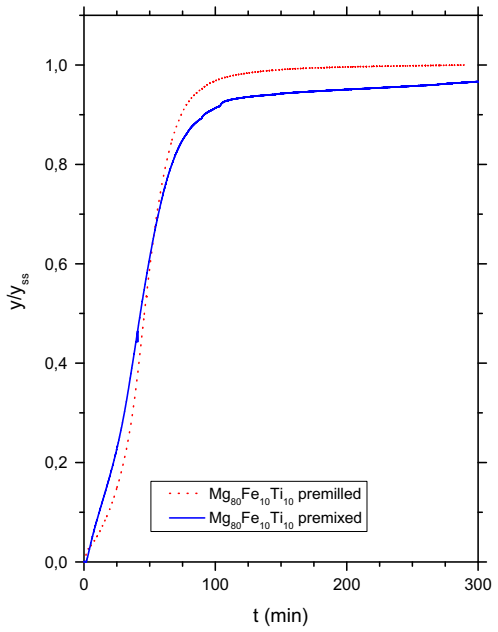


**Fig. 5.** Number of absorbed hydrogen atoms per metal atom $y = N_H/N_M$ normalized to its steady state value $y_{SS}$, as a function of milling time $t_m$ for samples MFT08 and MFT09.

**Table 1**
Sample description.

| Sample | Composition | Fe, Ti addition | Milling ambient | $x$ | $y$ |
|---|---|---|---|---|---|
| MFT04 | $Mg_{80}Fe_{10}Ti_{10}$ | Separately | $H_2$ | 0.10 | 1.81 |
| MFT05 | $Mg_{70}Fe_{15}Ti_{15}$ | Separately | $H_2$ | 0.15 | 1.71 |
| MFT06 | $Mg_{60}Fe_{20}Ti_{20}$ | Separately | $H_2$ | 0.20 | 1.99 |
| MFT07 | $Mg_{80}Fe_{10}Ti_{10}$ | Separately | $H_2$ | 0.10 | – |
| MFT08 | $Mg_{80}Fe_{10}Ti_{10}$ | As FeTi | Ar | 0.10 | – |
| MFT09 | $Mg_{80}Fe_{10}Ti_{10}$ | Premixed | Ar | 0.10 | – |
| MFT10 | $Mg_{80}Fe_{10}Ti_{10}$ | Premixed | $H_2$ | 0.10 | 1.86 |
| MFT11 | $Mg_{80}Fe_{10}Ti_{10}$ | As FeTi | $H_2$ | 0.10 | 1.57 |
| MFT12 | $Mg_{80}Fe_{10}Ti_{10}$ | As FeTi | $H_2$ | 0.10 | 1.57 |
| MFT13 | $Mg_{80}Fe_{10}Ti_{10}$ | Premixed | $H_2$ | 0.10 | 1.86 |

with smaller Fe content. The kinetic curves also show a faster initial stage, as compared with that observed in Mg–Fe samples, that may be associated with the prompt formation of $TiH_2$. This seems also to accelerate the formation of $MgH_2$. As an exception, the kinetic curve for samples MFT11 and MFT12, made from Mg and FeTi (premilled in Ar), shows a simpler sigmoidal shape corresponding to a single process (see Fig. 5): formation of $MgH_2$ catalyzed by FeTi. This is consistent with the fact that Fe and Ti are combined in the intermetallic FeTi and then no $TiH_2$ or $Mg_2FeH_6$ are expected to form, while some FeTi(H) may appear.

The hydrided samples were characterized by XRD and MS. We will first consider the results obtained on samples made from elemental Fe and Ti additives. The observed diffraction lines are broad as a result of the reduced grain size of the formed hydrides: about 10 nm according to the Scherrer formula. As shown in fig. 6 the main reflections present in most diffraction patterns are those coming from the complex ternary hydride $Mg_2FeH_6$ (cubic *Fm*3*m* structure) and from $TiH_2$, and in some samples (MFT04, MFT05) also from $MgH_2$ and Fe. As already pointed out, the $Mg_2FeH_6$ formation reaction is not always complete and some reactants are left, depending on the starting composition. The corresponding Mössbauer spectra were analyzed by least squares fitting of appropriate theoretical functions. All the measured spectra of as milled samples are similar (see Fig. 7) and could be reasonably well fitted with two or three components: (i) a singlet at $\delta = -0.125$ mm/s

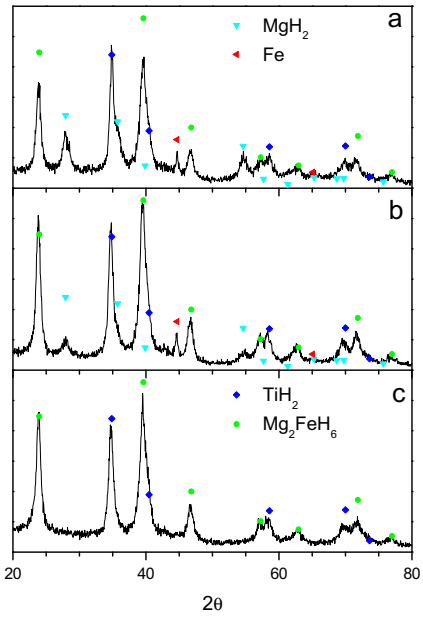


**Fig. 6.** X-ray diffraction patterns immediately after milling for (a) $Mg_{80}Fe_{10}Ti_{10}$ (MFT10), (b) $Mg_{70}Fe_{15}Ti_{15}$ (MFT05) and (c) $Mg_{60}Fe_{20}Ti_{20}$ (MFT06).

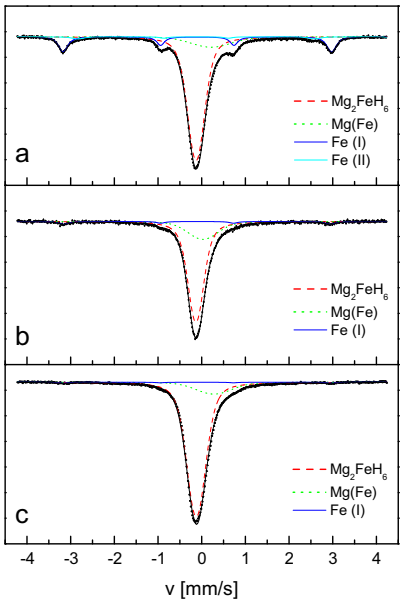


**Fig. 7.** Mössbauer spectra immediately after milling for (a) $Mg_{80}Fe_{10}Ti_{10}$ (MFT07), (b) $Mg_{70}Fe_{15}Ti_{15}$ (MFT05) and (c) $Mg_{60}Fe_{20}Ti_{20}$ (MFT06). Also shown the fitted curve and the associated subspectra. Fe(I) stands for normal Fe sites and Fe(II) for sites with one Mg nearest neighbour atom.

associated with the ternary hydride [6]; (ii) a broad singlet (or an unresolved doublet) centered at $\delta \approx 0.3$ mm/s that may be assigned to metastable Fe in Mg [23,24] and (iii) a magnetic sextet associated with the unreacted bcc Fe metal, present in those samples where the formation of the ternary hydride is not complete (MFT04, MFT07 and MFT05). Therefore, as shown concurrently by XRD and MS, for $x = 0.20$, almost all Fe is incorporated in $Mg_2FeH_6$. Considering present and previous results [12,25] we may conclude that there is an optimal Mg:Fe ratio, in the interval 2.5–3.5, for the accomplishment of that reaction. On his hand MS, due to its sensitivity to Fe environment, put in evidence that some Fe have been mechanically dissolved in Mg.

For samples made from FeTi the diffraction patterns indicate that the intermetallic is mostly preserved during alloying with Mg, either in Ar or $H_2$ (see Fig. 8a), although some Fe segregation may occur. Finally, in sample MFT09, the pattern gives evidence of the formation of fccTi as a result of the milling in Ar with Mg (see Fig. 8b). This metastable phase have been reported previously in mechanically alloyed Ti–Mg and Ti–Al mixtures [26,27]. The observed Mössbauer spectra depend on the ambient, Ar or $H_2$, used for the milling with Mg (Fig. 9). In the first case the spectrum is practically the same as that obtained for FeTi previous to the milling. While for the sample milled in $H_2$ a net increase in the isomer shift is evident ($\delta \approx -0.15$ mm/s) that must be associated to the dilution of some H in the FeTi matrix. Finally, the spectrum from sample MFT09 (not shown) indicates that there is an important dilution of Mg in Fe and that, besides FeTi, some $Fe_2Ti$ forms.

### 3.3. Thermally cycled samples

Typically each sample was discharged and recharged around ten times following the constant volume processes described above. The evolution of $P$ vs $T$ during the thermal $H_2$ desorption–absorption cycles at different starting pressures is shown in Fig. 10 for $Mg_{80}Fe_{10}Ti_{10}$ (MFT10) as representative of the general behavior. Except for the first desorption, immediately after mechanical synthesis, the curves and the associated ($T_i$, $P_i$) values are repetitive and show the expected $P(T)$ dependence. Although the observed desorption and absorption processes are not strictly isothermal, we may approximate the desorbed (absorbed) hydrogen quantity as proportional to the corresponding change in pressure $\Delta P$.

For the samples obtained by milling in Ar (MFT08 and MFT09) an activation process was necessary. The powders were similarly cycled in $H_2$ at constant volume, absorbing an increasing amount of $H_2$, till they attained a steady capacity (see Fig. 13). Almost full capacity is reached in sample MFT08 made from FeTi. Instead, for sample MFT09 a reduced capacity results with some pure Mg remaining, probably as a consequence of an adverse microstructure: formation of fccTi, $Fe_2Ti$ and Fe(Mg) during previous milling

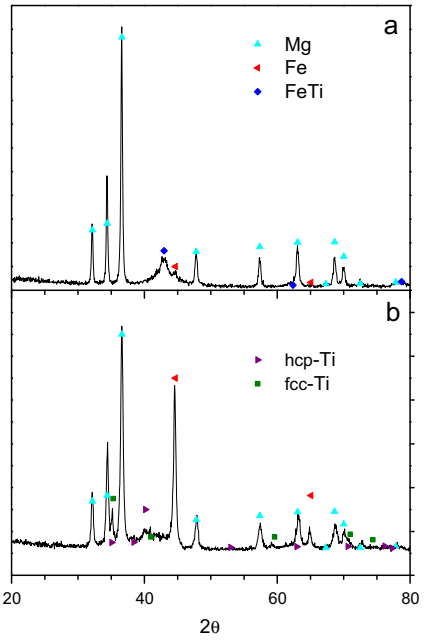


**Fig. 8.** X-ray diffraction patterns for samples milled in Ar (a) $Mg_{80}(FeTi)_{20}$ (MFT08) and (b) $Mg_{80}Fe_{10}Ti_{10}$ (MFT09).

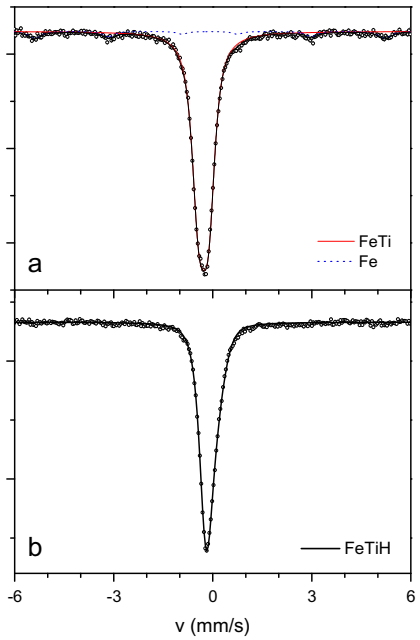


**Fig. 9.** Mössbauer spectra of $Mg_{80}(FeTi)_{20}$ samples milled in Ar (MFT08) or in $H_2$ atmosphere (MFT11). Also shown the fitted curve and the associated subspectra.

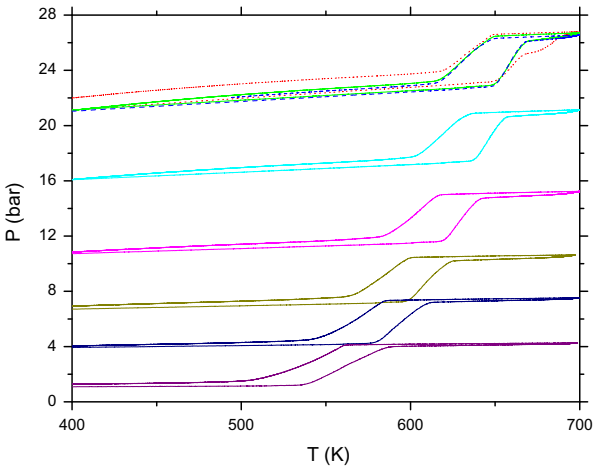


**Fig. 10.** Evolution of $P$ vs $T$ during the thermal $H_2$ desorption–absorption cycles for $Mg_{80}Fe_{10}Ti_{10}$ (MFT10) at different starting pressures.

in Ar. It is worth to note that the XRD pattern obtained after cycling shown an important fraction of Mg and traces of MgO.

The cycled samples were also characterized by XRD and MS. Generally the diffractograms show the presence of reflections coming mainly from tetragonal $MgH_2$, concurrently with the absence of lines from $Mg_2FeH_6$ (Fig. 11). There are also lines coming from bcc Fe or from the intermetallic FeTi and traces of Mg. Generally, the reflection peaks of the cycled samples diffractograms are sharper than those of the as milled ones indicating the crystallite mean size growth.

It is worth to note that one sample (MFT05), heated during the 4th cycle up to a higher $T$ (ca. 870 K), showed in the following cycles a considerably reduced sorption capacity. This may be attributed to the excessive Mg grain coarsening produced by the heating. The corresponding XRD pattern, taken after the cycling, shown the presence of MgO indicating the oxidation of the dehydrided sample during the subsequent handling.

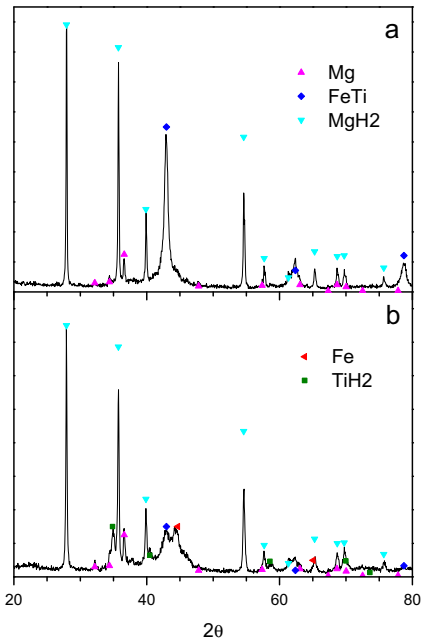


**Fig. 11.** X-ray diffraction patterns of samples (a) $Mg_{80}(FeTi)_{20}$ (MFT11) and (b) $Mg_{80}Fe_{10}Ti_{10}$ (MFT10) after cycling in $H_2$.

After thermal cycling the Mössbauer spectra became rather complex (see Fig. 12) and reveal the presence of several Fe-containing phases. Most of the spectra (MFT04, 05, 06, 07, 09, 10, 13) may be fitted with the same components in varying proportions: a main sextet (Fe) with a secondary one ascribed to Fe atoms with one Mg impurity as nearest neighbour; two central lines that can be described as a singlet and a doublet, assigned respectively to FeTi and $Fe_2Ti$ phases; and a broad central interaction not conclusively interpreted yet, but tentatively attributed to nanocrystalline FeTi complexes as those observed in films [15]. The singlet associated with $Mg_2FeH_6$ is not observed, confirming that the complex hydride does not form again after the first desorption. Concerning

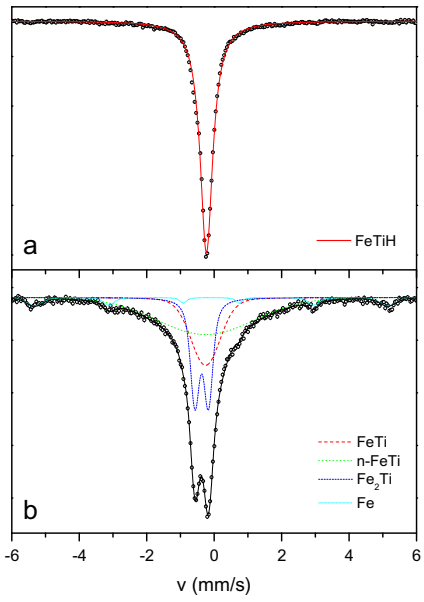


**Fig. 12.** Mössbauer spectra of samples (a) $Mg_{80}(FeTi)_{20}$ (MFT11) and (b) $Mg_{80}Fe_{10}Ti_{10}$ (MFT10) after cycling in $H_2$. Also shown the fitted curve and the associated subspectra.

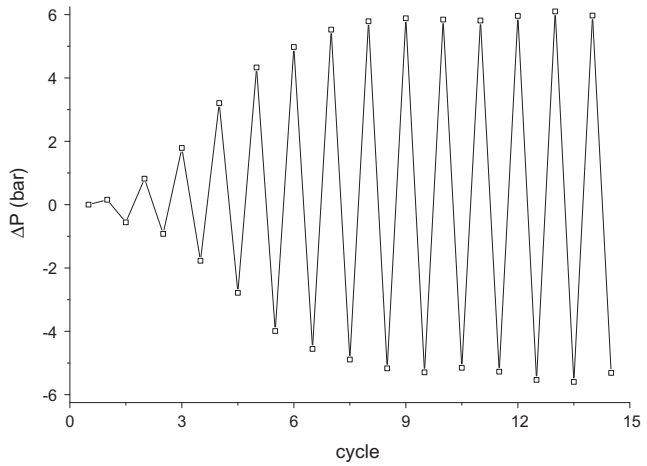


**Fig. 13.** Pressure change upon hydrogen desorption ($\Delta P > 0$) and absorption ($\Delta P < 0$) during successive heating–cooling cycles of 200 mg of $Mg_{80}(FeTi)_{20}$ milled in Ar (MFT08).

the $Fe_2Ti$ doublet, their characteristic parameters averaged over several samples were: isomer shift $\delta = 0.37$ mm/s and quadrupole splitting $\Delta = 0.41$ mm/s.

Additionally, we observed in the $P$ vs $T$ curves of samples containing FeTi, a faint shoulder preceding the main desorption effect. It occurs approximately at a temperature 25 K lower than $T_1$ and represents a $\Delta P$ of at most 0.05 bar (1.5% of that produced by the decomposition of $MgH_2$). Although the corresponding absorption effect is hard to observe in the cooling curves, the shoulder appears systematically, cycle after cycle, in the desorption ones and may be attributed to the reversible hydrogen release from interstitial FeTi(H).

### 3.4. Characteristic (T, P) values

As already mentioned, for the samples obtained by milling in $H_2$, the first desorption occurs at a higher temperature than the following ones. It corresponds to the dissociation of the complex hydride $Mg_2FeH_6$, which is not formed again as confirmed by XRD and MS. Putting aside these points, the remaining ($T_1$, $P_1$) and ($T_3$, $P_3$) values can be interpreted respectively as indicative of the start of the $MgH_2$-decomposition or $MgH_2$-formation in the cyclic desorption and absorption processes carried on. For each sample, the absorption and desorption points obey the relation $R \cdot \ln(P/P_o) = -\Delta G/T = \Delta S - \Delta H/T$, where $P_o$ is the standard pressure (100 kPa). This is illustrated in the vaṅt Hoff plot of Fig. 14 for one of the studied samples (MFT11), together with a fit with the above relation using a common value of the entropy change $\Delta S$ and different values of the enthalpy change $\Delta H$ for absorption and desorption. All the studied samples, including those that need activation, are well described by this relation, the fitted values of $\Delta H$ being comprised in the range −68.7 to −74.8 kJ/mol for absorption and 70.1–77.0 kJ/mol for desorption.

From the vaṅt Hoff plots, a reduction of about 40 K in the sorption temperature for a given pressure, as compared with pure $MgH_2$, is found for all the studied samples. This is still a smaller improvement than that found in thin films of the similar composition [15].

Finally, we observed that, through the present set of related samples, the entropy change $\Delta S$ seems to be correlated with the enthalpy change (see Fig. 15) displaying an entropy–enthalpy compensation phenomenon reported in many systems from a wide range of areas and lacking a well founded explanation [28].

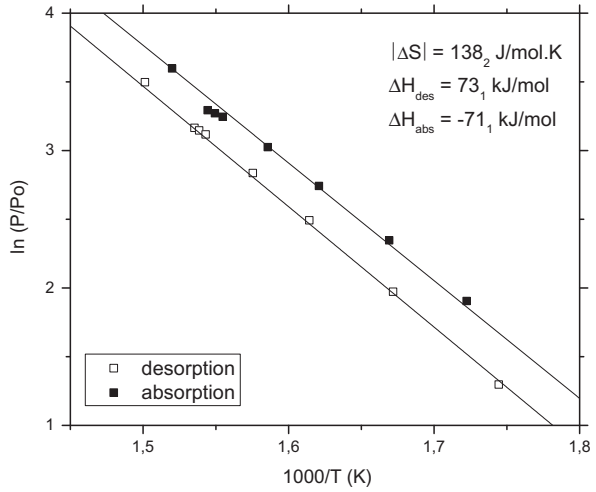


**Fig. 14.** Vañt Hoff plot, ln$P$ vs $1000/T(K)$, for $Mg_{80}(FeTi)_{20}$ (MFT11), fitted with a common $\Delta S$ value. The fitted $\Delta S$, $\Delta H_{des}$ and $\Delta H_{abs}$ values are also quoted.

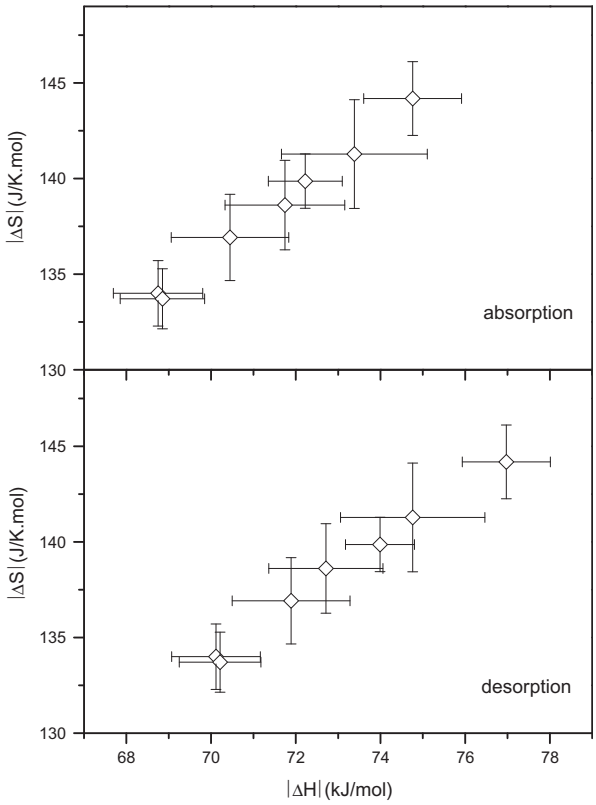


**Fig. 15.** $|\Delta S|$ – $|\Delta H|$ correlation for all the studied samples.

## 4. Conclusions

We have explored the mechanical synthesis of $Mg_{1-2x}Fe_xTi_x$ hydrides in powder form, with $x = 0.10$, 0.15, 0.20, and their response to repeated discharge–charge cycles.

The milling of Mg with Fe and Ti as additives in $H_2$ atmosphere leads to the formation of the hydrides $TiH_2$, $MgH_2$ and $Mg_2FeH_6$. The formation of the ternary hydride from $MgH_2$ is more or less complete depending on the starting composition. When the additives are under the form of intermetallic FeTi, the formation of $Mg_2FeH_6$ and $TiH_2$ is inhibited and besides $MgH_2$, the interstitial hydride FeTi(H) is formed.

Milling in Ar does not alter the intermetallic FeTi, but when Fe and Ti are included as separate components, it leads to the formation of the intermetallics FeTi and $Fe_2Ti$, and the metastable dilution of Mg in Fe, and that of Mg in fccTi. For the subsequent thermal hydriding of these samples an activation stage have to be overcame. Full capacity is thus obtained for the sample with the intermetallic FeTi, while that with elemental Fe and Ti exhibits limited capacity. This is caused by the formation of $Fe_2Ti$ and fccTi that, contrary to Fe, Ti and FeTi, do not catalyze the Mg hydriding, turning disadvantageous that fabrication route.

The behavior of mechanically hydrided samples under repeated hydrogen discharge–charge cycles was characterized by $P$ vs $T$ curves. Under our experimental conditions the ternary hydride $Mg_2FeH_6$ decomposes after the first heating and do not form anymore, leaving Fe separated from Mg. This feature might be used to obtain an specific microstructure if the decomposition could be driven in a controlled manner.

The subsequent charge and discharge processes in all samples consists basically on the formation and decomposition of $MgH_2$ differently catalyzed according to the state of the Fe and Ti additives, as Fe, $TiH_2$, FeTi/FeTi(H) or $Fe_2Ti$. While $TiH_2$ is stable within the $T$- and $P$-range employed, it seems that the presence of metallic Fe induces the formation of FeTi and $Fe_2Ti$ at expenses of $TiH_2$.

In summary we conclude that, unless there were added as intermetallic FeTi, the simultaneous presence of Fe and Ti does not imply a beneficial effect on their catalytic action in powder samples. On the contrary, Fe alone may constitute an interesting way to produce adequate microstructures under a controlled decomposition of mechanically produced $Mg_2FeH_6$ and $Ti/TiH_2$ have recently demonstrated to be a promising alternative [29].

## Acknowledgement

The financial support of CONICET, Argentina is gratefully acknowledged.

## References

[1] J. Huot, D.B. Ravnsbæk, J. Zhang, F. Cuevas, M. Latroche, T.R. Jensen, Mechanochemical synthesis of hydrogen storage materials, Prog. Mater. Sci. 58 (2013) 30–75.
[2] P. Selvam, B. Viswanathan, C.S. Swamy, V. Srinivasan, Magnesium and magnesium alloy hydrides, Int. J. Hydrogen Energy 11 (1986) 169–192.
[3] J. Huot, G. Liang, S. Boily, A. van Neste, R. Schulz, Structural study and hydrogen sorption kinetics of ball-milled magnesium hydride, J. Alloys Comp. 293–295 (1999) 495–500.
[4] G. Liang, R. Schulz, Synthesis of Mg–Ti alloy by mechanical alloying, J. Mater. Sci. 38 (2003) 1179–1184.
[5] G. Liang, J. Huot, S. Boily, A. van Neste, R. Schulz, Catalytic effect of transition metals on hydrogen sorption in nanocrystalline ball milled $MgH_2$–TM (TM = Ti, V, Mn, Fe and Ni) systems, J. Alloys Comp. 292 (1999) 247–252.
[6] J.J. Didisheim, P. Zolliker, K. Yvon, P. Fischer, J. Schefer, M. Gubelmann, A.F. Williams, Dimagnesium iron(II) hydride, $Mg_2FeH_6$, containing octahedral $FeH_6^4$ anions, Inorg. Chem. 23 (1984) 1953–1957.
[7] B. Bogdanovic, A. Reiser, K. Schlichte, B. Spliethoff, B. Tesche, Thermodynamics and dynamics of the Mg–Fe–H system and its potential for thermochemical thermal energy store, J. Alloys Comp. 345 (2002) 77–89.
[8] M. Khrussanovaa, E. Grigorovaa, I. Mitovb, D. Radeva, P. Pesheva, Hydrogen sorption properties of an Mg–Ti–V–Fe nanocomposite obtained by mechanical alloying, J. Alloys Comp. 327 (2001) 230–234.
[9] F.C. Gennari, F.J. Castro, J.J. Andrade Gamboa, Synthesis of $Mg_2FeH_6$ by reactive mechanical alloying: formation and decomposition properties, J. Alloys Comp. 339 (2002) 261–267.
[10] R.A. Varin, A. Li, A. Calka, D. Wexler, Formation and environmental stability of nanocrystalline and amorphous hydrides in the 2Mg–Fe mixture processed by controlled reactive mechanical alloying, J. Alloys Comp. 373 (2004) 270–286.
[11] J. Zhang, F. Cuevas, W. Zaidi, J.P. Bonnet, L. Aymard, J.L. Bobet, M. Latroche, Highlighting of a single reaction path during reactive ball milling of Mg and TM by quantitative $H_2$ gas sorption analysis to form ternary complex hydrides (TM = Fe Co, Ni), J. Phys. Chem. C 115 (2011) 4971–4979.
[12] L.A. Baum, M. Meyer, L. Mendoza-Zélis, The role of Fe during hydride formation in the Mg–Fe system: a Mössbauer investigation, Hyperfine Interact. 179 (2007) 61–65.

[13] L.A. Baum, M. Meyer, L. Mendoza-Zélis, Complex Mg-based hydrides obtained by mechanosynthesis: characterization and formation kinetics, Int. J. Hydrogen Energy 33 (2008) 3442–3446.
[14] L. Mendoza-Zélis, M. Meyer, L.A. Baum, Complex quaternary hydrides $Mg_2$(Fe, Co)Hy for hydrogen storage, Int. J. Hydrogen Energy 36 (2011) 600–605.
[15] B. Zahiri, C. Harrower, B.S. Amirkhiz, D. Mitlin, Rapid and reversible hydrogen sorption in Mg–Fe–Ti thin films, Appl. Phys. Lett. 95 (2009) 103114.
[16] P. Vermeulen, A. Ledovskikh, D. Danilov, P.H.L. Notten, Thermodynamics and kinetics of the thin film magnesium–hydrogen system, Acta Mater. 57 (2009) 4967–4973.
[17] R. Gremaud, C.P. Broedersz, A. Borgschulte, M.J. van Setten, H. Schreuders, M. Slaman, B. Dama, R. Griessen, Hydrogenography of $Mg_yNi_{1-y}$ $H_x$ gradient thin films: interplay between the thermodynamics and kinetics of hydrogenation, Acta Mater. 58 (2010) 658–668.
[18] W.P. Kalisvaart, C.T. Harrower, J. Haagsma, B. Zahiri, E.J. Luber, C. Ophus, E. Poirier, H. Fritzsche, D. Mitlin, Hydrogen storage in binary and ternary Mg-based alloys: a comprehensive experimental study, Int. J. Hydrogen Energy 35 (2010) 2091–2103.
[19] B.S. Amirkhiz, B. Zahiri, P. Kalisvaart, D. Mitlin, Synergy of elemental Fe and Ti promoting low temperature hydrogen sorption cycling of magnesium, Int. J. Hydrogen Energy 36 (2011) 6711–6722.
[20] H. Zhang, E.H. Kisi, Formation of titanium hydride at room temperature by ball milling, J. Phys.: Condens. Mater. 9 (1997) L185–L190.
[21] M.A. Bab, L. Mendoza-Zélis, A model for the kinetics of mechanically assisted gas–solid reactions, Scr. Mater. 50 (2003) 99–104.
[22] M.A. Bab, L.A. Baum, L. Mendoza-Zélis, Autocatalytic effects in the mechanically induced hydriding of refractory metals, Physica B 389 (2007) 193–197.
[23] A.M. van der Kraan, K.H.J. Buschow, $^{57}$Fe Mössbauer effect and magnetic properties in amorphous Fe-based alloys, Phys. Rev. B 25 (1982) 3311–3318.
[24] B. Sahoo, W. Keune, W. Sturhahn, T.S. Toellner, E.E. Alp, Atomic vibrational dynamics of amorphous Fe–Mg alloy thin films, J. Phys. Chem. Solids 66 (2005) 2263–2270.
[25] M. Meyer, L. Mendoza-Zélis, Mechanically alloyed Mg–Ni–Ti and Mg–Fe-Ti powders as hydrogen storage materials, Int. J. Hydrogen Energy 37 (2012) 14864–14869.
[26] C. Machio, D. Nyabadza, V. Sibanda, H.K. Chikwanda, Characterization of mechanically alloyed fcc Ti–Mg based powders, Powder Technol. 207 (2011) 387–395.
[27] D.L. Zhang, D.Y. Ying, Formation of fcc titanium during heating high-energy, ball-milled Al–Ti powders, Mater. Lett. 50 (2001) 149–153.
[28] K.F. Freed, Entropy–enthalpy compensation in chemical reactions and absorption: an exactly solvable model, J. Phys. Chem. B 115 (2011) 1689–1692.
[29] F. Cuevas, D. Korablov, M. Latroche, Synthesis, structural and hydrogenation properties of Mg-rich $MgH_2$–$TiH_2$ nanocomposites prepared by reactive ball milling under hydrogen gas, Phys. Chem. Chem. Phys. 14 (2012) 1200–1211.